A novel cryogenic scanning laser microscope tested on Josephson tunnel junctions

Holm, Jesper; Mygind, Jesper

Published in:
Review of Scientific Instruments

Link to article, DOI:
10.1063/1.1145288

Publication date:
1995

Document Version
Publisher's PDF, also known as Version of record

A novel cryogenic scanning laser microscope tested on Josephson tunnel junctions

J. Holm and J. Mygind
Physics Department, B309, Technical University of Denmark, DK-2800 Lyngby, Denmark and Danish Institute of Fundamental Metrology, B307, DK-2800 Lyngby, Denmark

(Received 12 October 1994; accepted for publication 14 June 1995)

A novel cryogenic scanning laser microscope with a spatial resolution of less than 5 μm has been designed for on-chip *in situ* investigations of the working properties of normal and superconducting circuits and devices. The instrument relies on the detection of the electrical response of the circuit to a very localized heating induced by irradiation with 675 nm wavelength light from a semiconductor laser. The hot spot is moved by a specially designed piezoelectric scanner sweeping the tip of a single-mode optical fiber a few μm above the circuit. Depending on the scanner design the scanning area can be as large as 50×500 μm^2 at 4.2 K. The microscope can be operated in the temperature range 2–300 K using a standard temperature controller. The central microscope body is mounted inside the vacuum can of a dip-stick-type cryoprobe. A damped spring system is used to reduce interference from extraneous mechanical vibrations. The microscope is integrated in a personal-computer-based data acquisition and control setup. © *1995 American Institute of Physics.*

I. INTRODUCTION

Interest in developing scanning electron and scanning laser microscopes for spatially resolved investigations of various semi-and superconducting devices at cryogenic temperatures has increased during the last few years.[1–4] Due to recent improvements in the fabrication technique of such devices, it has become increasingly difficult to combine the requirements of high resolution and high mechanical stability with the demands for a low noise environment, large scanning area, and robust and easy-to-operate overall design.

We have followed a new design strategy for our cryogenic scanning laser microscope (CSLM) where, in contrast to earlier designs,[1,5–8] the sample and the entire microscope including the piezo-scanner holding the glass fiber tip, the sample mounting stage, and the mechanical alignment system is maintained at low temperatures. This offers several advantages: thermal drift and fluctuations are reduced, the suppression of mechanical, electrical, and magnetic noise is improved, and *in situ* measurements can be made directly on the chip with the thin-film circuit in operation.

A laser diode kept at room temperature and mounted with an optical fiber, generates the laser beam. The beam emitted from the fiber tip, which is kept a few micrometers above the chip, locally heats the sample in a small circular area. Depending on the beam intensity, the optical reflection coefficient of the fiber tip and the sample, and the thermal properties of the sample, the temperature rise is typically several kelvin with an incident laser power of 10–100 μW. The spatial resolution depends on the beam radius and the thermal healing length of the sample[9,10] while, with our relatively low scan rates, the influence from the thermal relaxation time can be neglected. In experiments using a sample with a spatially extended all-niobium Josephson tunnel junction circuit deposited on a silicon chip, a resolution as low as 4 μm has been obtained.[10] This has to be compared to the thermal healing length of 1–3 μm commonly used[3] for setting an upper limit for the resolution. The physical model for the voltage response of the extended current-biased Josephson junctions used in the performance test of the microscope is discussed elsewhere.[10,11]

An elegant use of the controlled local heating is to drag-and-drop flux quanta into an annular Josephson junction[12] or a superconducting quantum interference device ring. Practically, this can be done by moving the ring across the hot spot enclosing a single flux quantum trapped in the small normal conducting region induced by the laser heating in the superconducting film.

Another application is the study of nonlinear transport phenomena in semiconductors at low temperatures by impact ionization breakdown of shallow impurities. The current density of such samples is inhomogeneous with highly conducting filamentary regions embedded in a weakly conducting environment. The resulting current exhibits complex temporal oscillations influenced by the various control parameters, e.g., temperature.[13]

The paper is organized as follows: The mechanical design of the microscope is given in Sec. II. Section III describes the electrical setup. Section IV contains the design and operation of the piezoelectric scanner. In Sec. V we discuss the physical model and the experimental results obtained on superconducting Josephson junctions used to demonstrate the performance of the microscope.

II. DESIGN OF MICROSCOPE AND CRYOPROBE

Immunity against external mechanical vibrations is vital for obtaining long-term stability and high spatial resolution. This is achieved by a compact and rigid design of the microscope body in combination with a suspension system of damped springs which mechanically isolates it from the outer housing.

A sketch of the CSLM is shown in Fig. 1. In principle it consists of three main mechanical parts: (i) a sample stage (items 5 and 6 in Fig. 1) with a coarse positioning system (not shown) and (ii) a piezoelectric scanner (item 4) mounted

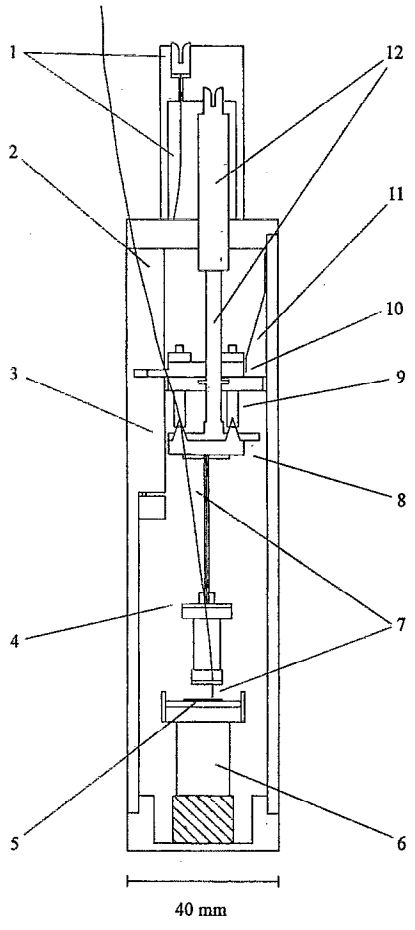

FIG. 1. The cryogenic scanning laser microscope. 1: Driver for wedge. 2: Flexible phosphorous bronze wire connection to wedge spindle. 3: Wedge housing. 4: Piezoelectric scanner. 5: Sample under investigation. 6: Sample stage with thermometers, heater, and thermal anchoring. 7: Optical fiber. 8–10: Aligning system carrying the piezo-scanner. 11: Leaf spring. 12: Differential screw for vertical adjustment.

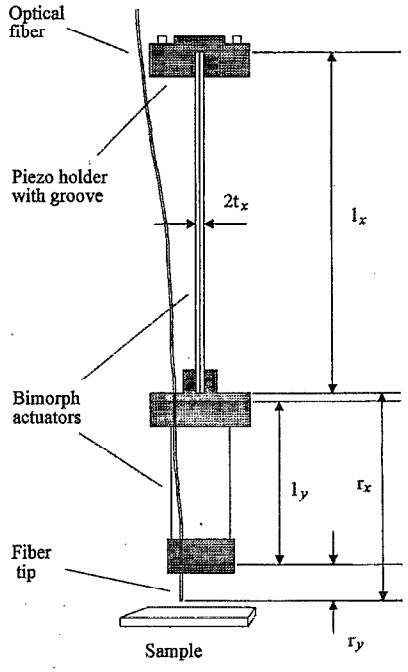

FIG. 2. The piezo-scanner consisting of two cantilever mounted bimorph actuators oriented perpendicular to one another. The dimensions of the scanner used in the text are in millimeters: $(l_x,t_x)=(42,0.35)$ and $(l_y,t_y)=(20,0.4)$.

onto (iii) a mechanical fine-alignment system (items 1–3 and 8–12). Not shown in Fig. 1 is the spring suspension system and the outer cylindrical vacuum can (50 mm o.d.) which constitutes the lower part of the cryoprobe (see below).

The sample chip, which might be as large as 20 mm × 20 mm is mounted on the copper sample stage (5) containing a bifilarly wound heater and two thermometers for temperature stabilization of the sample. The sample stage is thermally insulated from the cryoprobe can and all wires leading to the stage are thermally anchored to the copper block. It has been verified experimentally that neither the heater nor the thermal anchors produce disturbing magnetic fields at the position of the chip.

In order to reduce the vertical displacement of the fiber when thermally cycling the CSLM we have mounted the sample stage on a cylindrical Teflon block (cross hatched in Fig. 1). The length of the block is chosen so that the integral thermal expansion of the block, the copper stage, and the brass body of the outer part of the microscope approximately match the thermal contraction of the piezo-scanner with the mounted glass fiber. The Teflon block also provides the thermal isolation of the sample stage. The thermal compensation is purely static and it does not take into account the fact that parts with a large area-to-volume ratio and low-thermal capacitance parts cools (and heats) faster. In order to protect the sample and the fiber tip we always, after coarse aligning the system at room temperature, mechanically increase the tip–sample distance by several micrometers before cooling down. This is also done before returning to 300 K.

The simple coarse adjustment is provided for by two small screws (pitch=0.5 mm/turn) acting horizontally on the Teflon block which in turn is counteracted by a leaf spring.

In order to obtain a scanning range as large as 500 μm, we have implemented a novel design of the piezoelectric scanning element as shown in Fig. 2, consisting of two series-connected bimorph actuators mounted perpendicular to each other. Each actuator is made from two piezoelectric plates[14] glued together with their poling field oppositely directed using a low temperature epoxy (Stycast 1266).[15] Both sides of the plates are fully metallized so that an applied voltage establishes an electrical field perpendicular to the plate. The ends of the actuators are glued with Stycast 1266 into narrow grooves milled in a small bar of an insulating material. The optical fiber guiding the laser beam is mounted onto the last bar using GE 7031 varnish.

The mechanical vertical fine positioning of the fiber tip relative to the sample is performed by a differential screw moving the piezo-scanner 50 μm per turn. The horizontal fine positioning (in the $x-y$ plane) is performed by two spindle driven (pitch=0.4 mm/turn) wedges. The wedges are made so that one turn of the spindle moves the piezo-scanner 80 μm. In order to avoid hysteresis the moving of the two wedges as well as the fixture for the piezo-scanner is made against sets of leaf springs and ordinary springs. The maxi-

mum horizontal operating range of the system is 3.5 mm × 3.5 mm.

Since the mechanical fine-positioning system is kept at cryogenic temperatures it must be operated remotely from the top of the cryoprobe during the experimental runs. This is done by rotating spindles soldered to long thin walled stainless steel tubes mounted inside and thermally anchored to the 16-mm-diam central stainless steel tube of the cryoprobe. A special latching mesh gear allows the operator to withdraw the spindle after adjustment in order not to jeopardize the CLSM spring suspension system.

The CSLM is installed in a dip-stick-type cryoprobe which may be used in a helium cryostat or directly immersed in an ordinary (2-in.-diam neck) liquid helium transport vessel. The lower part of the cryoprobe is a cylindrical 300-mm-long can which, by a special reusable indium vacuum seal, is joined to a brass flange soldered on a long stainless steel tube leading to the room temperature top flange. Different cans are available: one with a long cylindrical solenoid used to supply a homogeneous magnetic field perpendicular to the chip, one with a cryoperm shield, and one with a superconducting shield. Two small Helmholtz coils can be mounted on the sample stage inside the microscope to provide a horizontal magnetic field at the position of the sample.

The top flange of the cryoprobe supports a metal box with built-in electronics, battery supplied low-noise preamplifiers, and low-pass filters. It also supports the various screws with rotary vacuum feedthroughs used for mechanically aligning the piezo-scanner as discussed above. A 50 Ω coaxial transmission line is mounted in the cryoprobe for exchange of microwave signals up to 26 GHz. Ultralow magnetic noise measurements are performed in a magnetically shielded glass cryostat installed in a shielded room.

The long stainless steel tube is equipped with a sliding joint which permits us to cycle the microscope between room temperature and the temperature of the coolant used in the cryostat. In fact we often simply lift the cryoprobe can out of the coolant to more quickly reach elevated experimental temperatures. This is particularly convenient for measurements on high-T_c superconducting samples.

The cryoprobe is a very practical device which allows us to mount and thermally cycle samples several times per day, thus keeping operational costs low. Mounted with the microscope and immersed in a 60 ℓ helium transportable storage vessel, cooling from 300 to 4 K takes less than 1 h with the use of 1.5 ℓ liquid helium. The evaporation rate during the experimental runs caused by the microscope is 30–40 ml/h, which is approximately half of the evaporation from the storage vessel itself.

In order to avoid interference from low-frequency mechanical vibrations typically originating from structural resonances of the building at frequencies below 50 Hz and with the corresponding amplitude reaching values of several micrometers, we have mechanically isolated the entire microscope from the cryoprobe by means of a simple suspension system consisting of three springs and a pair of support girders. With a total mass of 0.6 kg, this suspension system has a resonance frequency of approximately 1–2 Hz, thereby providing vibrational damping at higher frequencies. The relatively high resonance frequency which allows for a scan rate of 40 lines per s, also improves the immunity. Critical measurements are made in a cryostat which is placed on an optical table "floating" on air-filled tires.

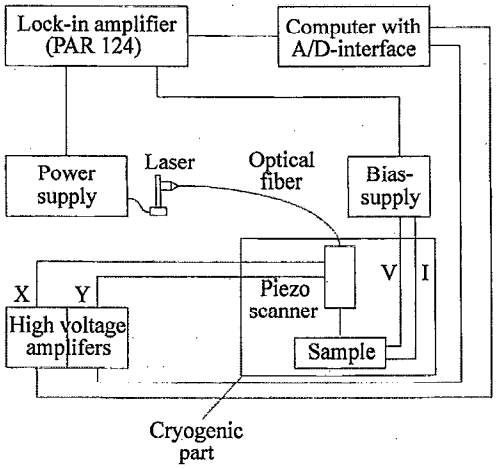

FIG. 3. Electronic setup for the CLSM. The semiconductor laser power is modulated by the reference oscillator in the lock-in amplifier. The modulation frequency is usually 4–8 kHz.

III. ELECTRONICS

A schematic diagram of the electronic setup is shown in Fig. 3. The moving of the piezo-scanner is controlled by a personal computer with a data acquisition system and a control adapter. The present setup generates images consisting of up to 256×256 pixels with an 8 bit resolution of the parameter under investigation. The signal from the standard D/A interface is fed to the input of the low-noise high voltage amplifiers able to deliver a voltage of ±200 V from two mutually inverted outputs with less than 1 mV_{pp} noise in a 20 kHz bandwidth.

The 675 nm wavelength light source is a commercially available (Toshiba Told 9211 AlGaInP) laser diode mounted with a single-mode optical fiber. The core diameter of the fiber is 3.5 μm, giving a mean field diameter around 4.5 μm at this wavelength. The output of the laser is usually modulated in the frequency range 4–8 kHz with a signal from the reference channel of a standard lock-in amplifier (Princeton Applied Research model 124) also used for detection of the response signal from the sample. After filtering the output signal from the lock-in is returned to the A/D interface and the computer for further processing. The maximum scan rate 40 lines/s is given by the software and not by the low frequency cutoff frequency of the piezo-scanner. This has been tested by monitoring the scan area on a chip with a known thin-film geometrical pattern as a function of scan rate. With a desired spatial resolution the signal averaging (i.e., the output filter) of the lock-in amplifier usually gives the highest usable scan rate of a few lines/s.

An important point of concern is the suppression of electromagnetic noise interfering with, e.g., ultrasensitive superconducting Josephson devices. This is done actively by using low-noise instrumentation, e.g., a battery-powered semiconductor laser and battery-powered isolation amplifiers, and

passively by careful filtering and shielding of all wires leading to the piezo-scanner and the device under test.

For single line scans on very noise-sensitive devices, such as superconducting Josephson devices, we employ an experimental procedure where the high-voltage amplifiers are operated manually (with input grounded) and the response signal is displayed on an analog XY recorder.

IV. OPERATION OF THE PIEZO-SCANNER

A. Principle of operation

By applying a voltage V to one outer electrode of the bimorph and $-V$ to the other and keeping the voltage of the common center electrode constant, the bimorph will bend, hereby moving the fiber tip horizontally with respect to the sample. The displacement of the fiber tip, $\Delta x_s(V)$ [or $\Delta y_s(V)$], can be found by assuming that the length of the center electrode remains unchanged while the outer electrodes get longer and shorter, respectively. The dilatation of the electrodes, Δl, is given by

$$\Delta l = d_{31} \frac{l}{t} V, \tag{1}$$

where l and t is the length and the thickness, respectively, of the single piezoelectric plate and d_{31} is the piezoelectric constant. Elementary geometry then gives

$$\Delta x_s(V) = \left(\frac{l_x}{t_x}\right)^2 \frac{d_{31}}{2} V\left(1 + \frac{2r_x}{l_x}\right), \tag{2}$$

where the subscript x refers to the bimorph in question, and r_x is the distance between the end of the bimorph and the sample (see Fig. 2). The scanning range in each direction is then $2\Delta x_s(V)$ and $2\Delta y_s(V)$, respectively, since the voltage of each electrode in our setup can be reversed utilizing the dual output of the high voltage amplifiers.

In this simple approach, we have not taken into account the part of the bimorphs glued into the grooves in the mounting bars. This may slightly reduce the scanning range, especially with relatively short actuators.

B. Scanner calibration

Each of the actuators will dilate if a voltage, V, is applied to both (common) center electrodes while the voltage of the outer electrodes is kept constant. The voltage-induced variation of the tip–sample distance can be measured by utilizing the optical (multiple) resonance effect between the nearly parallel flat fiber tip and the sample surface. As a function of V the laser power absorbed in the sample will be weakly modulated with periodicity $\lambda/2$, where λ is the laser wavelength. By using a small superconducting tunnel junction current biased in the thermal tunneling regime, we get a voltage response signal proportional to the absorbed power in the weak perturbation limit.[3]

Figure 4 shows the response voltage from the Josephson junction as a function of the center electrode voltage. From plotting the voltage positions of the maxima (minima) of the response we find a period corresponding to $\lambda/2 \sim 49$ V. Applying Eq. (1), we get

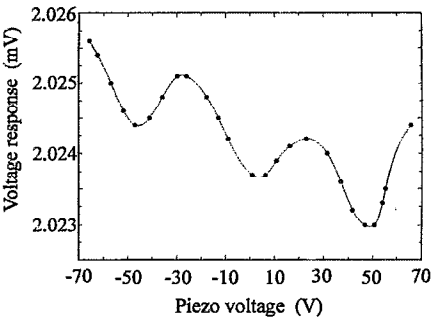

FIG. 4. Voltage response of a dc current biased long Josephson junction as a function of the voltage applied to the center electrode of both bimorphs. The weak modulation of the response signal is due to the variation in the optical resonance effect between the highly reflecting Nb surface of the sample and the plane cleaved fiber end caused by the dilatation of the piezo-scanner. $\lambda/2 \sim \Delta V \simeq 49$ V, where $\lambda = 675$ nm.

$$d_{31} = 47 \times 10^{-12} \text{ m/V} \tag{3}$$

which is in excellent agreement with the 5×10^{-11} m/V used for piezoelectric materials at 4.2 K.[16]

For the particular scanner with dimensions given in the caption of Fig. 2 the maximum scanning range for $V = \pm 200$ V is 300×35 μm^2. By using thinner and/or longer piezoplates for the actuators, it is possible to increase the scanning range for a given voltage span. We have constructed and tested scanners with a maximum scanning range exceeding 500 μm with $V = \pm 200$ V.

V. RESULTS AND DISCUSSION

We have performed experiments on long superconducting Josephson tunnel junctions. In these distributed devices the current density is spatially dependent. A local heating which changes the local current density results in a voltage response proportional to the local quasiparticle tunneling conductance provided the junction is constant current biased on the quasiparticle curve in its dc I-V characteristic.[3]

Figure 5(a) shows a sketch of the total scanned area where a part of a 5-μm-wide long Josephson junction embedded with a regular lattice of inhomogeneities of width 5 μm is seen. The inhomogeneities are placed in order to prevent quasiparticle tunneling through the oxide layer at these positions. Figure 5(b) shows the voltage response of the junction by scanning the area sketched in Fig. 5(a). The voltage response reflects the variation of the quasiparticle tunneling conductance caused by the presence of inhomogeneities.[3] Dark regions correspond to the minimum response, white to the maximum. The picture was recorded in 7 min with a scan rate of 1.2 lines/s. The calculated scanning range of 300 μm is seen to fit within experimental accuracy, since the distance between the individual inhomogeneities is 100 μm. Figure 5(b) also demonstrates the long term stability of the microscope, indirectly proving its immunity to extraneous electrical noise and mechanical vibrations. Figure 5(c) shows a profile of the response signal taken along the junction marked with arrows in Fig. 5(a). By measuring the width of the regular wells in the response signal and taking into account that the observed signal is folded with the Gaussian intensity distribution of the beam, it is

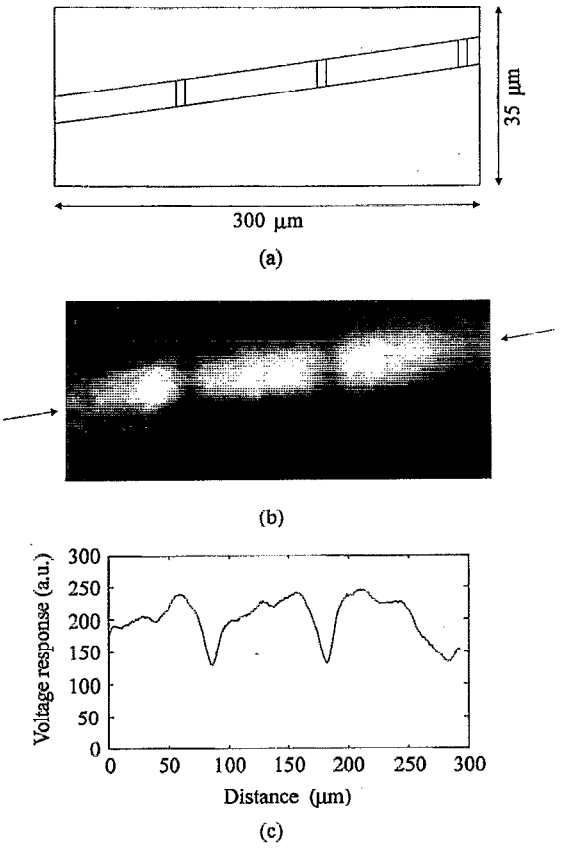

FIG. 5. (a) sketch of the area scanned with the CSLM. Part of an inhomogeneous 500-μm-long Josephson junction is seen. There is 100 μm between the 5-μm-wide silicon blocks in the oxide barrier of the junction. The junction itself is 5 μm wide. The scanning area is 300×35 μm^2 as calculated using Eq. (2) and the measured value of the piezoelectric constant d_{31}. (b) The CSLM image showing the voltage response of the junction when scanning the area sketched above. (c) Profile of the response signal in the figure. The profile is taken along the center of the junction (The light region).

possible to accurately determine the temperature distribution of the heated area as well as the lateral resolution defined here as the full width at half-maximum of this distribution.[17]

We plan to investigate the influence of the tip–sample distance on the spatial resolution. If we take into account the divergence of the laser beam presently emitted from the tip, the rough method used in cleaving the fiber, and the possible nonparallelism of the tip end surface relative to the sample, the observed variation (Fig. 4) of the response indirectly implies that the tip–sample distance is of the order a few μm. Fortunately we have not yet experienced a head-on impact which may damage the fiber tip. In the future we plan to improve the spatial resolution by mounting a very small hemispherical lens onto the tip and subsequently to correct for the spherical errors induced by the piezo-scanner. Thus in our opinion the application of the spherical lens is more feasible than to operate the CSLM in the near-field limit.

ACKNOWLEDGMENTS

B. F. Jørgensen, Electromagnetic Institute is acknowledged for help with the fiber preparation, and K. Brebøl, Ferroperm Ltd. for support of and information about piezoceramic materials. Finally we thank the Optics Group at the Physics Department for fruitful discussions and advice.

[1] Y. Y. Divin, F. Y. Nad, V. Y. Pokrovski, and P. M. Shadrin, IEEE Trans. Magn. **MAG-27**, 1101 (1991).
[2] D. Quenter *et al.*, Appl. Phys. Lett. **63**, 2135 (1993).
[3] R. Gross and D. Koelle, Rep. Prog. Phys. **57**, 651 (1994).
[4] A. Kittel (private communication).
[5] J. R. Lhota, M. Scheuermann, P. K. Kuo, and J. T. Chen, IEEE Trans. Magn. **MAG-19**, 1024 (1983).
[6] R. Gross, J. Bosch, H.-G. Wener, J. Fischer, and R. P. Huebener, Cryogenics **29**, 716 (1989).
[7] T. Doderer, H.-G. Wener, R. Moeck, C. Becker, and R. P. Huebener, Cryogenics **30**, 65 (1990).
[8] Y. Y. Divin and P. M. Shadrin, Phys. C **232**, 257 (1994).
[9] H. Pavlicek, L. Freytag, H. Seifert, and R. P. Huebener, J. Low Temp. Phys **56**, 237 (1984).
[10] J. Holm, Ph.D. thesis, Physics Department, Technical University of Denmark, October 1994.
[11] J. Holm and J. Mygind, IEEE Trans. Appl. Supercond. (in press).
[12] A. V. Ustinov, T. Doderer, R. P. Huebener, J. Mygind, V. A. Oboznov, and N. F. Pedersen, IEEE Trans. Appl. Supercond. **3**, 2287 (1993).
[13] M. Hirsch, A. Kittel, G. Flätgen, R. P. Huebener, and J. Parisi, Phys. Lett. A **186**, 157 (1994).
[14] The piezoelectric plates were purchased from Ferroperm ltd., Kvistgaard, Denmark.
[15] Trademark of Emerson & Cuming, Inc., Canton, MA 02021.
[16] Information material from Channel Industries, Inc., Santa Barbara, CA 93111, Vernitron Piezoelectric Division, Morgan Matroc Inc., Bedford, OH 44146, and Stavely Sensors Inc., East Hartford, CT 06108. See also K. G. Vandervoort, R. K. Zasadzinski, G. G. Galicia, and G. W. Crabtree, Rev. Sci. Instrum. **64**, 896 (1993).
[17] J. Holm and J. Mygind (unpublished).